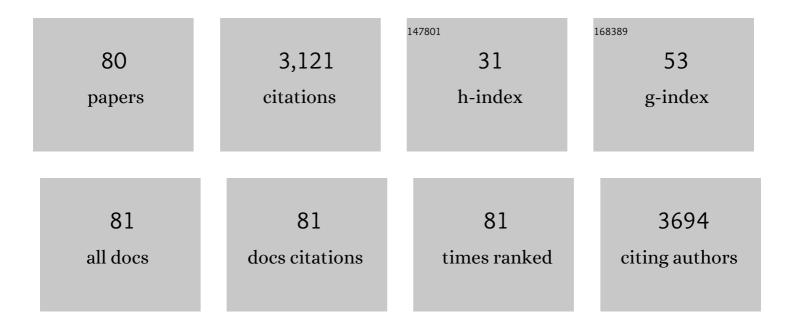
Xiao-hua Zhang

List of Publications by Year in descending order

Source: https://exaly.com/author-pdf/4042235/publications.pdf Version: 2024-02-01



#	Article	IF	CITATIONS
1	A label-free photoelectrochemical biosensor with ultra-low-background noise for lead ion assay based on the Cu2O-CuO-TiO2 heterojunction. Analytica Chimica Acta, 2022, 1195, 339456.	5.4	17
2	Highly Selective Photoelectrochemical Assay of Arsenate Based on Magnetic Co ₃ O ₄ –Fe ₃ O ₄ Cubes and the Negative-Background Signal Strategy. Analytical Chemistry, 2022, 94, 1874-1881.	6.5	23
3	One-step integration of amorphous RuB _{<i>x</i>} and crystalline Ru nanoparticles into B/N-doped porous carbon polyhedra for robust electrocatalytic activity towards the HER in both acidic and basic media. Journal of Materials Chemistry A, 2022, 10, 4181-4190.	10.3	16
4	Zinc–Air Battery-Assisted Self-Powered PEC Sensors for Sensitive Assay of PTP1B Activity Based on Perovskite Quantum Dots Encapsulated in Vinyl-Functionalized Covalent Organic Frameworks. Analytical Chemistry, 2022, 94, 9844-9850.	6.5	27
5	Active site and intermediate modulation of 3D CoSe2 nanosheet array on Ni foam by Mo doping for high-efficiency overall water splitting in alkaline media. Chemical Engineering Journal, 2021, 417, 128055.	12.7	60
6	Peptide Cleavage-Mediated and Environmentally Friendly Photocurrent Polarity Switching System for Prostate-Specific Antigen Assay. Analytical Chemistry, 2021, 93, 1076-1083.	6.5	39
7	Sensitive Dual-Mode Biosensors for CYFRA21-1 Assay Based on the Dual-Signaling Electrochemical Ratiometric Strategy and "On–Off–On―PEC Method. Analytical Chemistry, 2021, 93, 6801-6807.	6.5	74
8	A photocurrent-polarity-switching biosensor for highly selective assay of mucin 1 based on target-induced hemin transfer from ZrO2 hollow spheres to G-quadruplex nanowires. Biosensors and Bioelectronics, 2021, 192, 113547.	10.1	17
9	Highly Selective and Sensitive microRNA-210 Assay Based on Dual-Signaling Electrochemical and Photocurrent-Polarity-Switching Strategies. Analytical Chemistry, 2021, 93, 14272-14279.	6.5	39
10	A novel signal-off photoelectrochemical biosensor for M.Sssl MTase activity assay based on GQDs@ZIF-8 polyhedra as signal quencher. Biosensors and Bioelectronics, 2020, 150, 111861.	10.1	53
11	Highly Selective and Sensitive Photoelectrochemical Sensing Platform for VEGF165 Assay Based on the Switching of Photocurrent Polarity of CdS QDs by Porous Cu ₂ O-CuO Flower. Analytical Chemistry, 2020, 92, 1189-1196.	6.5	99
12	CuO–ZnO heterojunction derived from Cu2+-doped ZIF-8: A new photoelectric material for ultrasensitive PEC immunoassay of CA125 with near-zero background noise. Analytica Chimica Acta, 2020, 1099, 75-84.	5.4	35
13	DNA-linked CdSe QDs/AGQDs "Z-scheme―system: Ultrasensitive and highly selective photoelectrochemical sensing platform with negative background signal. Sensors and Actuators B: Chemical, 2020, 305, 127480.	7.8	22
14	Sensitive photoelectrochemical assay of Pb ²⁺ based on DNAzyme-induced disassembly of the "Z-scheme―TiO ₂ /Au/CdS QDs system. Chemical Communications, 2020, 56, 8261-8264.	4.1	22
15	3D amorphous NiFe LDH nanosheets electrodeposited on <i>in situ</i> grown NiCoP@NC on nickel foam for remarkably enhanced OER electrocatalytic performance. Dalton Transactions, 2020, 49, 4896-4903.	3.3	32
16	Spontaneous deposition of Ir nanoparticles on 2D siloxene as a high-performance HER electrocatalyst with ultra-low Ir loading. Chemical Communications, 2020, 56, 4824-4827.	4.1	39
17	Label-free and near-zero-background-noise photoelectrochemical assay of methyltransferase activity based on a Bi ₂ S ₃ /Ti ₃ C ₂ Schottky junction. Chemical Communications, 2020, 56, 5799-5802.	4.1	40
18	Target-induced photocurrent-polarity switching: a highly selective and sensitive photoelectrochemical sensing platform. Chemical Communications, 2019, 55, 8939-8942.	4.1	16

#	Article	IF	CITATIONS
19	A sensitive photoelectrochemical assay of miRNA-155 based on a CdSe QDs//NPC-ZnO polyhedra photocurrent-direction switching system and target-triggered strand displacement amplification strategy. Chemical Communications, 2019, 55, 2182-2185.	4.1	43
20	A sensitive photoelectrochemical methyltransferase activity assay based on a novel "Z-scheme―CdSe QD/afGQD heterojunction and multiple signal amplification strategies. Chemical Communications, 2019, 55, 8166-8169.	4.1	12
21	Low-cost high-performance hydrogen evolution electrocatalysts based on Pt-CoP polyhedra with low Pt loading in both alkaline and neutral media. Dalton Transactions, 2019, 48, 8920-8930.	3.3	29
22	A new photoelectrochemical immunosensor for ultrasensitive assay of prion protein based on hemin-induced photocurrent direction switching. Biosensors and Bioelectronics, 2019, 132, 55-61.	10.1	33
23	Facile solution synthesis of FeN _x atom clusters supported on nitrogen-enriched graphene carbon aerogels with superb electrocatalytic performance toward the oxygen reduction reaction. Journal of Materials Chemistry A, 2019, 7, 25557-25566.	10.3	29
24	Fe and S co-doped N-enriched hierarchical porous carbon polyhedron as efficient non-noble-metal electrocatalyst toward oxygen reduction reaction in both alkaline and acidic medium. Electrochimica Acta, 2019, 298, 570-579.	5.2	54
25	A new electrochemical immunoassay for prion protein based on hybridization chain reaction with hemin/G-quadruplex DNAzyme. Talanta, 2018, 182, 292-298.	5.5	23
26	A label-free and blocker-free photoelectrochemical strategy for highly sensitive caspase-3 assay. Chemical Communications, 2018, 54, 4830-4833.	4.1	24
27	High-performance non-enzymatic catalysts based on 3D hierarchical hollow porous Co3O4 nanododecahedras in situ decorated on carbon nanotubes for glucose detection and biofuel cell application. Analytical and Bioanalytical Chemistry, 2018, 410, 2019-2029.	3.7	12
28	A new electrochemical immunosensor for sensitive detection of prion based on Prussian blue analogue. Talanta, 2018, 179, 726-733.	5.5	34
29	A new photoelectrochemical biosensor for ultrasensitive determination of nucleic acids based on a three-stage cascade signal amplification strategy. Analyst, The, 2018, 143, 2799-2806.	3.5	27
30	Co ₃ O ₄ –Au Polyhedra: A Multifunctional Signal Amplifier for Sensitive Photoelectrochemical Assay. Analytical Chemistry, 2018, 90, 9480-9486.	6.5	70
31	A new electrochemical aptasensor for sensitive assay of a protein based on the dual-signaling electrochemical ratiometric method and DNA walker strategy. Chemical Communications, 2018, 54, 10359-10362.	4.1	60
32	Preparation of NiCoP Hollow Quasi-Polyhedra and Their Electrocatalytic Properties for Hydrogen Evolution in Alkaline Solution. ACS Applied Materials & amp; Interfaces, 2017, 9, 5982-5991.	8.0	217
33	Hierarchical porous carbon materials prepared by direct carbonization of Al-PCP as a Pt-catalyst support for the oxygen reduction reaction. New Journal of Chemistry, 2017, 41, 7432-7437.	2.8	3
34	Template-synthesis and electrochemical properties of urchin-like NiCoP electrocatalyst for hydrogen evolution reaction. Electrochimica Acta, 2017, 249, 301-307.	5.2	29
35	Triple-Helix Molecular Switch Electrochemical Ratiometric Biosensor for Ultrasensitive Detection of Nucleic Acids. Analytical Chemistry, 2017, 89, 8830-8835.	6.5	116
36	Nitrogen-Doped Porous Carbon-ZnO Nanopolyhedra Derived from ZIF-8: New Materials for Photoelectrochemical Biosensors. ACS Applied Materials & Interfaces, 2017, 9, 42482-42491.	8.0	130

XIAO-HUA ZHANG

#	Article	IF	CITATIONS
37	Sensitive electrochemical assay of alkaline phosphatase activity based on TdT-mediated hemin/G-quadruplex DNAzyme nanowires for signal amplification. Biosensors and Bioelectronics, 2017, 87, 970-975.	10.1	77
38	Exonuclease III–assisted cascade signal amplification strategy for label-free and ultrasensitive electrochemical detection of nucleic acids. Biosensors and Bioelectronics, 2017, 87, 732-736.	10.1	62
39	A label-free and cascaded dual-signaling amplified electrochemical aptasensing platform for sensitive prion assay. Biosensors and Bioelectronics, 2016, 85, 471-478.	10.1	24
40	A high-performance bioanode based on a nitrogen-doped short tubular carbon loaded Au nanoparticle co-immobilized mediator and glucose oxidase for glucose/O ₂ biofuel cells. RSC Advances, 2016, 6, 29142-29148.	3.6	7
41	Quantitative fluorescence kinetic analysis of NADH and FAD in human plasma using three- and four-way calibration methods capable of providing the second-order advantage. Analytica Chimica Acta, 2016, 910, 36-44.	5.4	21
42	A novel electrochemical aptasensor for bisphenol A assay based on triple-signaling strategy. Biosensors and Bioelectronics, 2016, 79, 22-28.	10.1	72
43	An electrochemical biosensor for sensitive detection of Hg ²⁺ based on exonuclease III-assisted target recycling and hybridization chain reaction amplification strategies. Analytical Methods, 2016, 8, 2106-2111.	2.7	21
44	Smart protein biogate as a mediator to regulate competitive host-guest interaction for sensitive ratiometric electrochemical assay of prion. Scientific Reports, 2015, 5, 16015.	3.3	30
45	Carbon nanotube–ionic liquid composite gel based high-performance bioanode for glucose/O ₂ biofuel cells. Analytical Methods, 2015, 7, 5060-5066.	2.7	8
46	One-pot synthesis of PtRh/Ĵ²-CD-CNTs for methanol oxidation. International Journal of Hydrogen Energy, 2015, 40, 14866-14874.	7.1	15
47	Platinum Nanoparticles Encapsulated in Nitrogenâ€Doped Mesoporous Carbons as Methanolâ€Tolerant Oxygen Reduction Electrocatalysts. ChemElectroChem, 2015, 2, 404-411.	3.4	28
48	Ultrasonic cavitation assisted hydrogen implosion synthesis of Pt nanoparticles/nitrogen-doped graphene nanohybrid scrolls and their electrocatalytic oxidation of methanol. Ionics, 2015, 21, 1287-1294.	2.4	7
49	Ultrasensitive Electrochemical Detection of Nucleic Acids Based on the Dual-Signaling Electrochemical Ratiometric Method and Exonuclease III-Assisted Target Recycling Amplification Strategy. Analytical Chemistry, 2015, 87, 7291-7296.	6.5	143
50	A flexible trilinear decomposition algorithm for three-way calibration based on the trilinear component model and a theoretical extension of the algorithm to the multilinear component model. Analytica Chimica Acta, 2015, 878, 63-77.	5.4	17
51	Solid-state grinding/low-temperature calcining synthesis of carbon coated MnO ₂ nanorods and their electrochemical capacitive property. New Journal of Chemistry, 2015, 39, 4731-4736.	2.8	12
52	Synthesis of high-concentration B and N co-doped porous carbon polyhedra and their supercapacitive properties. RSC Advances, 2015, 5, 77527-77533.	3.6	15
53	A new electrochemical aptasensor based on electrocatalytic property of graphene toward ascorbic acid oxidation. Talanta, 2015, 134, 699-704.	5.5	13
54	A ratiometric electrochemical biosensor for sensitive detection of Hg 2+ based on thymine–Hg 2+ –thymine structure. Analytica Chimica Acta, 2015, 853, 242-248.	5.4	111

XIAO-HUA ZHANG

#	Article	IF	CITATIONS
55	Nanomaterials as signal amplification elements in DNA-based electrochemical sensing. Nano Today, 2014, 9, 197-211.	11.9	134
56	Amplified impedimetric DNA sensor based on graphene oxide–phenylboronic acid for sensitive detection of bleomycins. New Journal of Chemistry, 2014, 38, 2284.	2.8	12
57	Highly-selective electrochemical determination of catechol based on 3-aminophenylboronic acid-3,4,9,10-perylene tetracarboxylic acid functionalized carbon nanotubes modified electrode. Analytical Methods, 2014, 6, 718-724.	2.7	26
58	A ratiometric electrochemical aptasensor for sensitive detection of protein based on aptamer–target–aptamer sandwich structure. Journal of Electroanalytical Chemistry, 2014, 732, 61-65.	3.8	32
59	Electrochemical determination of bleomycins based on dual-amplification of 4-mercaptophenyl boronic acid-capped gold nanoparticles and dopamine-capped gold nanoparticles. Analytical Methods, 2014, 6, 6893.	2.7	10
60	A simple label-free electrochemical aptasensor for dopamine detection. RSC Advances, 2014, 4, 52250-52255.	3.6	45
61	Chemometrics-enhanced high performance liquid chromatography-diode array detection strategy for simultaneous determination of eight co-eluted compounds in ten kinds of Chinese teas using second-order calibration method based on alternating trilinear decomposition algorithm. Journal of Chromatography A, 2014, 1364, 151-162.	3.7	24
62	Self-assembly synthesis of a hierarchical structure using hollow nitrogen-doped carbon spheres as spacers to separate the reduced graphene oxide for simultaneous electrochemical determination of ascorbic acid, dopamine and uric acid. Analytical Methods, 2013, 5, 3591.	2.7	32
63	Sensitive electrochemical sensor of anthracene-9-carbonxylic acid using an electropolymerized film modified glassy carbon electrode. Analytical Methods, 2013, 5, 1881.	2.7	1
64	Simultaneous electrochemical detection of ascorbic acid, dopamine and uric acid based on nitrogen doped porous carbon nanopolyhedra. Journal of Materials Chemistry B, 2013, 1, 2742.	5.8	166
65	A combined theoretical and experimental study for the chiral discrimination of naproxen enantiomers by molecular modeling and second-order standard addition method. Analytical Methods, 2013, 5, 710.	2.7	11
66	Fast HPLC-DAD quantification of nine polyphenols in honey by using second-order calibration method based on trilinear decomposition algorithm. Food Chemistry, 2013, 138, 62-69.	8.2	54
67	Chemometrics-assisted excitation-emission fluorescence spectroscopy for simultaneous determination of ethoxyquin and tert-butylhydroquinone in biological fluid samples. Science China Chemistry, 2013, 56, 664-671.	8.2	1
68	Second-order calibration applied to quantification of two active components of Schisandra chinensis in complex matrix. Journal of Pharmaceutical Analysis, 2012, 2, 241-248.	5.3	7
69	Measuring estriol and estrone simultaneously in liquid cosmetic samples using second-order calibration coupled with excitation–emission matrix fluorescence based on region selection. Analytical Methods, 2012, 4, 222-229.	2.7	16
70	Carbonization of ionic liquid polymer-functionalized carbon nanotubes for high dispersion of PtRu nanoparticles and their electrocatalytic oxidation of methanol. Journal of Materials Chemistry, 2012, 22, 13085.	6.7	33
71	Enhanced Electrochemical Sensing for Persistent Organic Pollutants by Nanohybrids of Graphene Nanosheets that are Noncovalently Functionalized with Cyclodextrin. ChemPlusChem, 2012, 77, 844-849.	2.8	8
72	One-pot synthesis of highly dispersed palladium nanoparticles on acetylenic ionic liquid polymer functionalized carbon nanotubes for electrocatalytic oxidation of glucose. Journal of Solid State Electrochemistry, 2012, 16, 759-766.	2.5	24

XIAO-HUA ZHANG

#	Article	IF	CITATIONS
73	Preparation of polyaniline–tin dioxide composites and their application in methanol electro-oxidation. Journal of Solid State Electrochemistry, 2010, 14, 169-174.	2.5	34
74	PMo12-functionalized Graphene nanosheet-supported PtRu nanocatalysts for methanol electro-oxidation. Journal of Solid State Electrochemistry, 2010, 14, 2267-2274.	2.5	38
75	Ethanol electrooxidation on platinum particles dispersed on poly(neutral red) film. Journal of Applied Electrochemistry, 2008, 38, 1665-1670.	2.9	5
76	Synthesis and thermal stability of a novel cycloaliphatic epoxy resin system. Journal of Applied Polymer Science, 2008, 108, 518-522.	2.6	3
77	Toughening of cycloaliphatic epoxy resin by multiwalled carbon nanotubes. Journal of Applied Polymer Science, 2008, 110, 1351-1357.	2.6	38
78	Synthesis and characterization of epoxy film cured with phosphorous-containing phenolic resin. Journal of Applied Polymer Science, 2007, 104, 3813-3817.	2.6	5
79	Synthesis of novel phosphorous-containing biphenol, 2-(5,) Tj ETQq1 1 0.784314 rgBT /Overlock 10 Tf 50 507 Td flame-retardant in epoxy resin. Journal of Applied Polymer Science, 2006, 102, 3842-3847.	(5-dimeth 2.6	iyl-4-phenyl-2 27
80	Facilely Hierarchical Growth of N-Doped Carbon-Coated NiCo ₂ O ₄ Nanowire Arrays on Ni Foam for Advanced Supercapacitor Electrodes. ACS Sustainable Chemistry and Engineering, 0, , .	6.7	4